JOURNAL OF PROPULSION AND POWER
Vol. 30, No. 5, September–October 2014

Combustion of Vaporized Kerosene in Supersonic Model Combustors with Dislocated Dual Cavities

Taichang Zhang,* Jing Wang,* and Xuejun Fan†
State Key Laboratory of High Temperature Gas Dynamics, Chinese Academy of Sciences, 100190 Beijing, People's Republic of China
and
Peng Zhang‡
Hong Kong Polytechnic University, Kowloon, Hong Kong, People's Republic of China

DOI: 10.2514/1.B35096

Supersonic combustion of vaporized kerosene in a Mach 2.5 model combustor with a total temperature of 1500 K and a total pressure of 1.3 MPa was experimentally investigated for an optimal integration of the cavity-based flameholder and the fuel injection scheme. A novel design of a supersonic model combustor consisting of a two-staged fuel injection system and dislocated dual cavities was proposed to improve the combustor performance, including the combustion efficiency, flame stabilization, combustor "unstart," and heat release distribution. Specifically, a large number of experiments were performed to systematically investigate the effects of fuel injection distribution, which is controlled by varying the injector spacing and the fuel equivalence ratio, on the static pressure distribution, thrust increment, lean blowout limit, wall temperature distribution, and combustor unstart characteristics. The results show that there exists an optimal range of injector spacing to obtain enhanced combustion performance while avoiding the combustion unstart. Furthermore, the equal fuel injection with an overall equivalence ratio of 0.5 for the two injectors was found to result in the optimal static pressure distribution and hence the largest thrust increment.

Nomenclature

C	=	cavity
I	=	injector
M	=	Mach number
P	=	pressure, MPa
Q	=	mass flow rate, kg/s
T	=	temperature, K
x	=	streamwise location from the combustor entrance
ΔX	=	spacing between the first- and second-stage injectors
$\Delta\Gamma$	=	increment of specific thrust, m/s
Φ	=	equivalence ratio

Subscripts

f	=	fuel
inj	=	injection
s	=	static condition
w	=	wall
0	=	stagnant condition
1	=	first stage
2	=	second stage

I. Introduction

THERE are several important advantages to using onboard liquid fuel as a combustor coolant in scramjet propulsion. First, the high flight Mach number of a scramjet-propelled vehicle results in a high stagnation temperature in the supersonic combustor and in turn a high wall temperature, which can, however, be effectively reduced by flowing the cold liquid fuel around the hot combustor wall to absorb the excessive heat. The liquid fuel will be accordingly heated to a certain extent before it is injected into the combustor. Second, it is very challenging to directly burn a liquid fuel in a supersonic flow because the flow residence time may be not sufficient enough for atomizing and vaporizing the liquid fuel, mixing the fuel vapor with air, and igniting and burning the fuel–air mixture. As the liquid fuel is heated up to a vaporized state (supercritical or cracked), its atomization and vaporization can be completely avoided and an enhanced combustion performance can be expected. Actually, many previous experimental studies [1–4] have demonstrated that the use of vaporized hydrocarbon fuels holds the potential of enhancing fuel–air mixing and promoting overall combustion performance.

It is widely recognized that the performance of a supersonic combustor is substantially influenced by the flameholding and fuel injection schemes [5,6]. Thus, it is expected that the scramjet combustor fueled with vaporized hydrocarbon fuels has its specific optimal integration of flameholding and fuel injection schemes. The cavity-based flameholder has been widely used and extensively studied [6–11] due to its advantages in stabilizing the flame while minimizing the total pressure loss and eliminating the requirement for additional thermal protection to the flameholder. Based on the consideration, only the cavity-based flameholding scheme was adopted in the present study.

Many early studies were focused on understanding the flameholding mechanism of a single cavity in supersonic combustors and optimizing the cavity design [4,8,12,13]. Only a few studies have been performed by using multiple cavities in supersonic combustors [2,11,14,15]. Fan et al. [2] studied the combustion of supercritical kerosene in a supersonic combustor equipped with two pairs of integrated injector/cavity modules, which are installed in tandem along the flowpath. Collatz et al. [14] experimentally and numerically investigated the combustion performance of using a pair of cavities located on opposite walls of the supersonic combustor. Such opposite dual-cavity design was used in the Hypersonic International Flight Research and Experimentation scramjet combustor [11], because it is able to significantly improve the overall combustion performance. Regardless of these studies, several important design issues for an

Presented as Paper 2012-3762 at the 48th AIAA/ASME/SAE/ASEE Joint Propulsion Conference & Exhibit, Atlanta, GA, 30–1 August 2012; received 23 July 2013; revision received 7 November 2013; accepted for publication 9 December 2013; published online 23 April 2014.

*Associate Professor, Institute of Mechanics, No. 15 Beisihuanxi Road. Member AIAA.

†Professor, Institute of Mechanics, No. 15 Beisihuanxi Road; xfan@imech.ac.cn. Member AIAA (Corresponding Author).

‡Assistant Professor, Department of Mechanical Engineering, No. 11 Yucai Road.

optimal supersonic combustor design, such as the relative axial positions between the two cavities and between the fuel injection and the cavities, have not been studied and hence were considered in the present study.

A two-staged fuel injection scheme, in which fuel is injected into the combustor from two injection locations, was adopted in the present study. The recent study [16] on the blowout limits of supercritical kerosene injected from the upstream of a cavity in a supersonic combustor shows that the overall equivalence ratio between the lean and rich blowout limits is generally located in the range of 0.3–0.8. Further increasing the fuel flow rate by using single-staged injection is prohibited to avoid the combustor unstart [17], which is a result of the pressure rise at the combustor entrance due to the locally excessive heat release. The two-staged fuel injection [18–22] should be able to distribute the combustion heat release and hence avoid the combustor unstart. Previous work [20,21] indicates that the interaction of two-staged injection is not obvious in the case of hydrogen. However, it is worthy to study the interaction in the case of kerosene due to the distinct characteristics of mixing and chemical reaction. Moreover, the influence of the injector interval on the interaction of two-stage injections, especially in terms of the flame stability, is not very clear.

A previous experiment [23] shows that the penetration depth of vaporized kerosene in a supersonic combustor can be as large as 40 mm. It is reasonable to expect that the injection from one side of the combustor wall cannot consume the oxygen near the other side if the height of the combustor is larger than the penetration depth. The two-staged injection from opposite sides of the combustor is proposed to improve the combustion efficiency because it holds the potential of completely consuming all the oxygen in the airflow. Moreover, the two-staged injection from opposite sides of the combustor is assumed to be able to lessen the nonuniformity of the heat flux on the combustor wall and hence increase the reliability of the combustor.

There are several advantages to installing the dual injectors away from each other with one certain spacing. The combustion of the first-staged fuel can provide a higher flow temperature and an active radical pool for the combustion of the second-staged fuel. The combustion of the second-stage injected fuel can in turn reduce the local flow velocity, increase the pressure in the combustor, and consequently promote the flame stabilization. The mechanism of the second-staged injection is analogous to that of a mechanical or gas dynamic throttling, which has been proven to be able to enhance the ignition and the flame stabilization [24]. Furthermore, a better pressure distribution and higher thrust may be attained in a staged supersonic combustor [18–22].

The interaction between the fuel injection and the flameholding cavity is another important issue that needs to be considered to optimize the supersonic combustor design. Previous studies [16] on the effect of the injection location on the blowout limit of vaporized kerosene demonstrated that injection from the wall upstream of a cavity results in a much wider range of fuel equivalence ratio for stable combustion than does the injection from the rear part of the cavity floor. Consequently, the two fuel injectors in the present experiments are always installed in the upstream of the corresponding cavities.

Based on the preceding considerations, the combustion characteristics of vaporized kerosene in a supersonic model combustor with two-staged fuel injection integrated with dislocated dual cavities were experimentally investigated in the present study. A Mach 2.5 model combustor was tested in the airflow with a total temperature of 1500 K and total pressure of 1.3 MP. The study was focused on investigating the effects of the integrated fuel injection/cavity design on the combustion performance, including the flame stabilization, engine unstart, and heat release distribution. In this paper, we shall present the experimental setup and the typical operation results in Sec. II, followed by the results and discussion in Sec. III.

II. Experimental Setup and Operation

A. Direct-Connect Supersonic Combustor

All the experiments in the present study were conducted in a direct-connect wind-tunnel facility, which consists of an air supply system, a Mach 2.5 multipurpose supersonic model combustor, and a fuel delivery and heating system. The vitiated air, which is supplied by burning H_2 in air with oxygen replenishment, has a stagnation temperature of 700–2200 K and a stagnation pressure of 0.6–4.5 MPa. Figure 1a shows the supersonic model combustor with a total length of 1500 mm, which consists of a 400-mm-long isolator of nearly constant cross section, a 800-mm-long divergent section with a 2.0 deg expansion angle, and a 300-mm-long divergent section with a 5.3 deg expansion angle. The dimensions at the combustor entry are 50 mm in height and 70 mm in width. Two cavity modules (C-1 and C-2) are installed on opposite sides of the combustor. Each cavity module has a depth of 12 mm, an aft ramp angle of 45 deg, and an overall length-to-depth ratio of 7. Cavity module 1 is located at

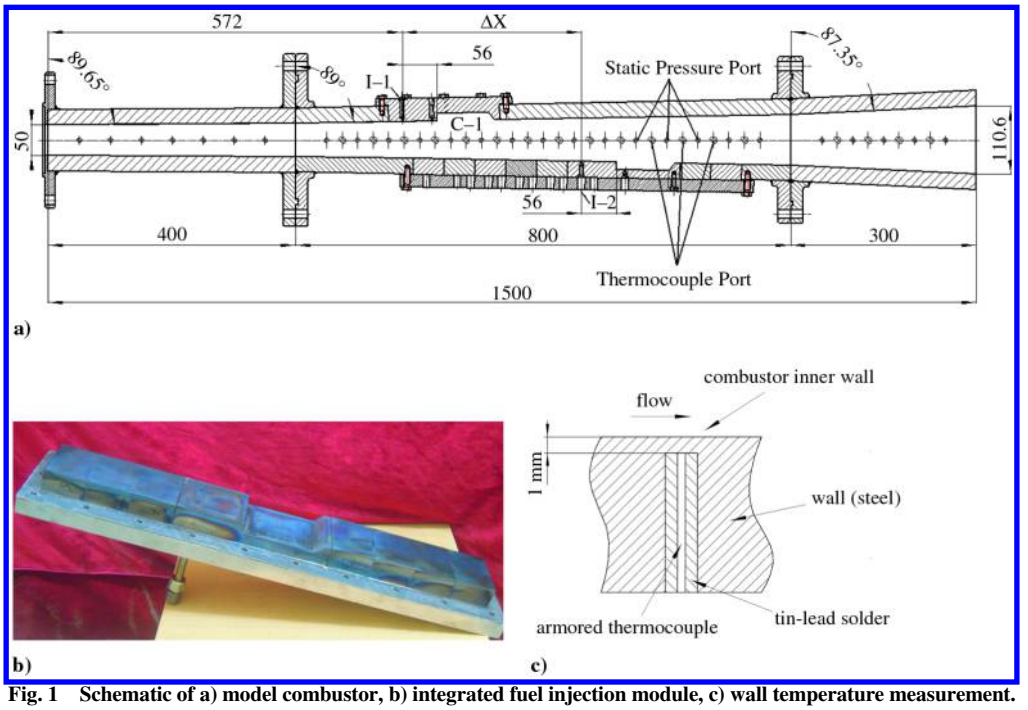

Fig. 1 Schematic of a) model combustor, b) integrated fuel injection module, c) wall temperature measurement.

628 mm downstream of the isolator entry defined as $x = 0$. The location of C-2 can be varied by assembling C-2 with seven other identical wall modules, each of which has a length of 50 mm and a width of 70 mm, as shown in Fig. 1b. Two orifices of 1.5 mm in diameter located upstream of C-1 are used for the injection of pilot hydrogen. Each of the two fuel injectors (I-1 and I-2) have two orifices of 2.8 mm in diameter, with I-1 located at 56 mm upstream of C-1 (i.e., 48 mm upstream of the pilot hydrogen) and I-2 at 56 mm upstream of C-2. The length-to-depth ratio of the cavity used in present work refers the previous work [7,8,25], whereas other design parameters, such as the injector diameter and the injector-to-cavity interval, are based on the previous work from the authors' group [2,22]. The spacing between two fuel injectors is accordingly variable in the range of 40–390 mm through varying the relative location of C-1 and C-2. A 50 J/pulse park plug (Xuzhou Combustion Control Technology Co., Ltd., China) is installed on one of the cavity floors for ignition.

B. Measurement System

The stagnation pressure of the airflow is measured by using a CYB-10S pressure transducer (accuracy ±0.1%, Beijing Zhong-HangJiDian Technology Co., Ltd., China). The static pressure distribution in the axial direction is determined by using the Motorola MPX2200 pressure transducers installed with 50 mm spacing along the centerline of the sidewalls of the model combustor.

The stagnation temperature of the airflow is measured by using a type-B thermocouple. The wall temperature is measured by using the K-type thermocouple armored with a stainless steel sheath with 1.0 mm diameter. The thermocouple is installed in a hole, which is in the combustor wall and filled with tin–lead solder, as shown in Fig. 1c. The tip of the armored thermocouple closely contacts the bottom of the hole and is 1.0 mm apart from the inner wall surface. The thermocouples are installed with 50 mm spacing between each, along the centerline of the model combustor sidewall from $x =$ 475 mm to the combustor exit at $x = 1500$ mm. Although it is recognized that the measured temperature is not necessarily the actual wall temperature because of the temperature redistribution over the tin–lead soldering, the variation of combustion heat release along the combustor can be qualitatively reflected by the wall temperature measurement.

The entire test rig is mounted upright on a platform. Three weight sensors (Shanghai TM, model NS-TH3) are equilaterally spaced and connected in series to support the platform and measure the thrust. This system has a maximum force reading of 7500 N with a full-scale uncertainty of 0.05%.

C. Kerosene Delivery and Heating System

Supercritical kerosene at a temperature of 760 ± 10 K and a pressure of 3–6 MPa was prepared in a two-staged kerosene heating and delivering system [26], as shown in Fig. 2. The first stage is a storage heater that can heat the kerosene of 0.8 kg up to 570 K with negligible coking deposits. The second stage is a continuous heater, which is used to rapidly heat kerosene to a desired temperature within a few seconds.

Before each experiment, the kerosene in a storage cylinder is pumped into the first-stage heater by a piston driven by high-pressure nitrogen gas. Two pneumatic valves (Swagelok, models SS6UM and SS10UM), which are installed at the exits of the first- and second-stage heaters, respectively, are employed to turn on/off the two heaters sequentially. As the kerosene in the first-stage heater reaches a desired temperature at a given pressure, it is pressed into the second-stage heater and heated up to the working temperature before being injected into the model combustor. Two groups of K-type thermocouples (Omega, model KMQSS-0.032E) are installed on the surface of the heater tubes or inserted into them. These thermocouples are used to monitor the fuel temperature distribution in the heating system and subsequently used as a feedback to control the system. Steady fuel temperature and pressure at the exit of the heating system are achieved and maintained during the whole experiment.

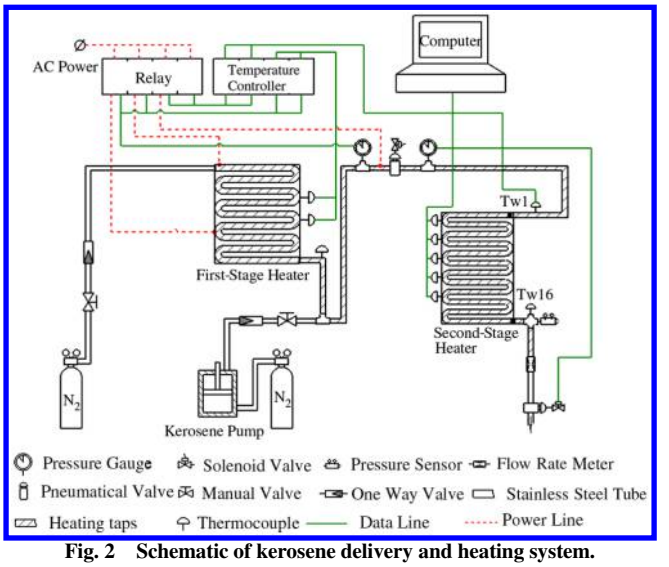

Fig. 2 Schematic of kerosene delivery and heating system.

The mass flow rate of the supercritical kerosene is controlled and measured by sonic nozzles, which are installed at the exit of the second-stage heater. The calibration of the nozzles has been described in detail in earlier work [2]. The mass flow rate of each sonic nozzle is determined based on the fuel temperature and pressure P_f measured in the immediate upstream of the nozzle. The precise control of fuel temperature at 760 ± 10 K ensures the accuracy of the mass flow rate, because it is not sensitive to the temperature in the range. Considering the measurement uncertainties of the throat area, the fuel pressure, and the fuel temperature, the overall uncertainty for the measured mass flow rate is less than 5%. The fuel pressure is measured immediately upstream the injector and used as the injection pressure P_{inj}.

D. Typical Experimental Operation

Figure 3 shows the time sequences of the pilot hydrogen pressure, the supercritical kerosene pressure, the total pressure, and temperature of the flow in a typical experiment. The equivalence ratio of the pilot hydrogen used in this experiment is about 0.08. The supersonic airflow, the pilot hydrogen, and the supercritical kerosene start at 2.9, 3.6, and 4.2 s, respectively. The pilot hydrogen is shut down completely at 5.0 s. The airflow and the kerosene are shut down at 9.0 s and delay about 0.5 s due to the operation of the valves. Figure 3 shows that both the inlet airflow and the kerosene flow keep steady during the experiment.

Figure 4 shows the evolution of the thrust in the experiment. The thrust increase in the time interval of 2.9–3.6 s is purely due to the gas dynamic effect of the supersonic flow because no combustion happens during the time interval. Thrust should be subtracted as a reference value from the thrusts obtained after the fuel injection and

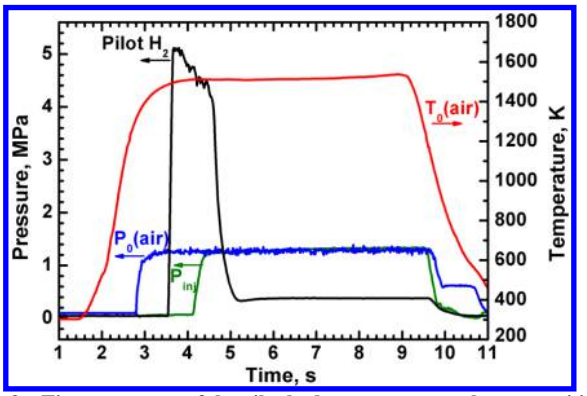

Fig. 3 Time sequences of the pilot hydrogen pressure, the supercritical kerosene pressure, the stagnation temperature, and pressure of the airflow in a typical experiment.

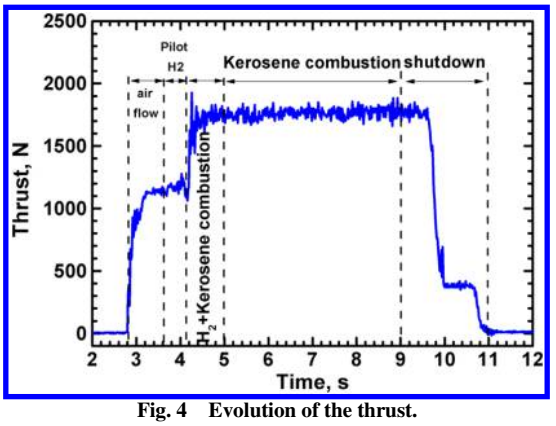

Fig. 4 Evolution of the thrust.

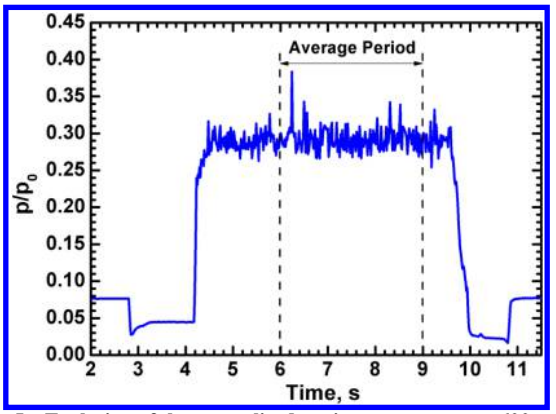

Fig. 5 Evolution of the normalized static pressure at $x = 600$ mm.

combustion. The slight increase of the thrust during 3.6–4.2 s is due to the combustion of the pilot hydrogen. During the time interval of 4.2–5.0 s, the vaporized kerosene is ignited by the pilot hydrogen flame and, subsequently, the combustion of kerosene and hydrogen causes a further thrust increase. The thrust maintains nearly steady from the shutdown of the pilot hydrogen at 5.0 s to the end of the experiment at 9.5 s. To eliminate the influence of the pilot hydrogen combustion and the possibly unsteady combustion of kerosene after their shutdown at 5 and 9 s, respectively, the average of thrust is calculated by using the data during the time interval of 6.0–9.0 s. The specific thrust increment $\Delta\Gamma$, which is defined as the thrust increment per unit of mass flow rate of air, can hence be determined.

Figure 5 shows the evolution of the static pressure measured at $x = 600$ mm normalized by the stagnation air pressure in the experiment. Similarly, we used the measured static pressure in the time interval of 6–9 s to calculate the average pressure, which will be used in the following discussion.

III. Results and Discussions

In this section, the effects of the spacing ΔX between the two-staged fuel injectors on the static pressure distribution, thrust, and wall temperature distribution will be examined first. The effects of the second-staged injection on the flame stabilization will be then investigated for two typical cases of $\Delta X = 190$ and 390, respectively. Finally, the effects of the ratio of the fuel flow rates of the two-staged injection on the static pressure distribution, thrust, and wall temperature distribution will be investigated for the case of $\Delta X = 190$. All the experimental conditions reported in the paper are listed in Tables 1–3, respectively.

Table 1 Experimental conditions and measured specific thrust increments

	Vitiated air			Kerosene					
Figure	P_0, MPa	T_0, K	Q, kg/s	P_f, MPa	P_{inj}, MPa	T_f, K	Φ_1/Φ_2	ΔX, mm	$\Delta\Gamma$, m/s
6–11	1.30	1493	1.509	4.88	1.30	757	0.49/0.51	40	520
	1.30	1507	1.501	4.88	1.30	760	0.49/0.51	90	473
	1.30	1494	1.509	4.88	1.30	756	0.50/0.52	140	443
	1.26	1485	1.464	4.98	1.35	754	0.51/0.53	190	415
	1.30	1509	1.500	5.00	1.35	757	0.504/0.527	190	423
	1.29	1482	1.499	4.89	1.30	756	0.50/0.52	190	440
	1.30	1509	1.495	4.89	1.30	751	0.50/0.52	240	413
	1.30	1541	1.484	4.87	1.30	752	0.50/0.52	290	412
	1.30	1501	1.506	4.89	1.30	756	0.49/0.51	340	408
	1.31	1503	1.516	4.89	1.33	753	0.49/0.51	390	419

Table 2 Experimental conditions and flame stabilization

	Vitiated air			Kerosene					
Figure	P_0, MPa	T_0, K	Q, kg/s	P_f, MPa	P_{inj}, MPa	T_f, K	Φ_1/Φ_2	ΔX, mm	Flame stabilization
12	1.28	1507	1.478	4.77	1.18	760	0.269/0.0	190	Stabilized
	1.28	1512	1.475	4.44	1.06	758	0.251/0.0	190	Marginal
	1.28	1495	1.484	4.19	0.99	755	0.237/0.0	190	Blowout
13	1.29	1508	1.488	4.62	0.67	758	0.16/0.37	190	Blowout
	1.27	1468	1.481	4.91	0.73	760	0.172/0.398	190	Stabilized
	1.27	1462	1.489	3.18	0.69	760	0.178/0.182	190	Stabilized
	1.29	1514	1.485	2.88	0.63	756	0.162/0.166	190	Blowout
	1.28	1483	1.489	4.60	0.66	763	0.162/0.471	190	Blowout
	1.27	1490	1.475	4.44	0.73	758	0.173/0.501	190	Stabilized
14	1.30	1495	1.507	4.29	1.03	755	0.237/0.0	390	Blowout
	1.28	1484	1.485	4.72	1.16	761	0.265/0.0	390	Marginal
	1.29	1514	1.490	4.85	1.22	756	0.275/0.0	390	Stabilized
	1.30	1551	1.478	3.75	0.86	759	0.211/0.216	390	Stabilized
	1.30	1541	1.483	4.03	0.93	763	0.225/0.231	390	Stabilized
	1.30	1531	1.495	3.59	0.82	754	0.203/0.208	390	Blowout
	1.28	1489	1.487	5.83	0.94	759	0.204/0.471	390	Blowout
	1.29	1535	1.475	4.12	0.94	759	0.233/0.44	390	Stabilized

Table 3 Experimental conditions and measured specific thrust increments

	Vitiated air			Kerosene					
Figure	P_0, MPa	T_0, K	Q, kg/s	P_f, MPa	P_{inj}, MPa	T_f, K	Φ_1/Φ_2	ΔX, mm	$\Delta\Gamma$, m/s
15	1.27	1482	1.478	4.44	1.42	755	0.363/0.64	190	350
	1.26	1485	1.464	5.00	1.35	754	0.51/0.53	190	415
	1.30	1511	1.499	4.47	1.70	755	0.636/0.36	190	404
16	1.30	1509	1.500	5.00	1.35	757	0.504/0.527	190	423
	1.29	1478	1.504	4.67	1.44	755	0.493/0.636	190	422
	1.29	1477	1.504	4.76	1.46	755	0.502/0.709	190	428
	1.29	1528	1.477	6.17	2.23	759	0.50/0.0	190	283

A. Effects of Spacing Between the Two-Staged Injectors

To experimentally investigate the influence of the dislocated, parallel two-staged injection on the combustion performance, the injectors were installed so that the first injector was always fixed at $x = 572$ mm on the one side of the combustor and the second injector was installed on the other side of the combustor, varying from $x = 612$ to 962 mm with a 50 mm increment. The fuel equivalence ratios are 0.50 and 0.52 for the first- and second-staged injector, respectively. The detailed experimental conditions are listed in Table 1.

Figure 6 shows the variation of the normalized static pressure along the combustor for different spacing ΔX between the two-staged injectors. Several observations can be made from the results. First, at a large injector spacing, such as $\Delta X = 390$ mm, two peak values on the static pressure curve can be clearly identified around $x = 650$ and 1050 mm, which indicates the existence of two relatively independent combustion zones downstream of the two injectors located at $x = 572$ and 962 mm, respectively. As ΔX decreases, the second peak gradually moves to and eventually merges with the first one. Consequently, the first peak value increases and at the same time moves downstream due to the strengthening effect of the second combustion zone. Furthermore, the leading edge of the pressure rise moves upstream with the decrease of ΔX, as shown in Fig. 6. This is a result of the increasing upstream propagation of the static pressure due to the stronger and more concentrated combustion. It is noted that, for $\Delta X = 40$, the static pressure at the entrance of the isolator is lifted above 0.05, which implies the entry Mach number has been changed due to the propagation of pressure beyond the isolator, and hence the combustor unstart occurs.

The suppression of a spatially distributed heat release on the pressure rise in the isolator can be understood in theory as follows. Assuming the internal flow in a combustor, a steady, generalized one-dimensional frictionless flow with variable cross-sectional area A and variable total temperature T_t due to heat addition, the streamwise variation of Mach number is given by [27]

$$\frac{\mathrm{d}M}{\mathrm{d}x} = M\left(\frac{1+(\gamma-1/2)M^2}{1-M^2}\right)\left\{-\left(\frac{1}{A}\frac{\mathrm{d}A}{\mathrm{d}x}\right)+\frac{1+\gamma M^2}{2}\left(\frac{1}{T_t}\frac{\mathrm{d}T_t}{\mathrm{d}x}\right)\right\} \tag{1}$$

The axial distribution of the static pressure can be accordingly determined by

$$p(x) = p_{\mathrm{in}}\frac{A_{\mathrm{in}}}{A(x)}\frac{M_{\mathrm{in}}}{M(x)}\sqrt{\frac{T(x)}{T_{\mathrm{in}}}} \tag{2}$$

where

$$T(x) = T_{\mathrm{in}}\frac{T_t(x)}{T_{t\mathrm{in}}}\left[\frac{1+(\gamma-1)/2M_{\mathrm{in}}^2}{1+(\gamma-1)/2M^2(x)}\right] \tag{3}$$

where the subscript "in" denotes the isolator entrance.

If a given amount of heat release is spread out in space, the decreasing of the Mach number along the streamwise position x (as $\mathrm{d}M/\mathrm{d}x < 0$) will be smaller because the gradient of total temperature decreases compared with the case of concentrated heat release. Consequently, $T(x)/T_{\mathrm{in}}$ and $M_{\mathrm{in}}/M(x)$ will be smaller and the pressure rise will be smaller under the condition of distributed heat release, suggesting that unstart can be suppressed for well-distributed heat release. The conclusion is consistent with the experimental observations of the present study.

A one-dimensional calculation has been performed to assess the flowfield in the combustor. The one-dimensional model has been reported in detail [28]. Briefly, the measured profile of the static pressure was first fitted and subsequently used as an input to calculate axial profiles of Mach number, total pressure, total temperature, and so on. Figure 7 shows the calculated average Mach number profile for the cases of Fig. 6. It can be seen that thermal choking occurs in all the cases, and the average flow speed in most of the combustion section is less than sonic speed. Moreover, there are two choking points for each case, and both locations propagate approximately linearly upstream with the decrease of the interval, as shown in Fig. 8, which demonstrates that the location of thermal choking is significantly influenced by the injector interval.

Figure 9 shows the variation of corresponding specific thrust increment with respect to the different spacings between the two-staged injectors. The specific thrust increment moderately increases from 408 to 473 m/s as the spacing ΔX decreases from 390 to 90 mm, with an approximate plateau in the range of $\Delta X =$

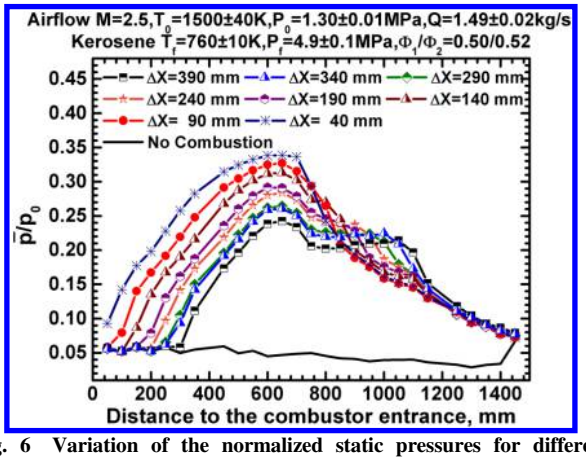

Fig. 6 Variation of the normalized static pressures for different spacings between injectors.

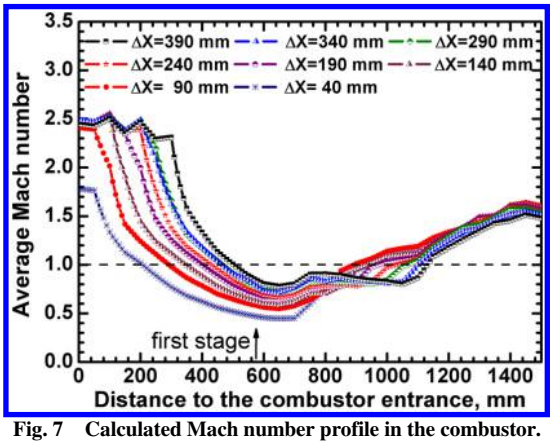

Fig. 7 Calculated Mach number profile in the combustor.

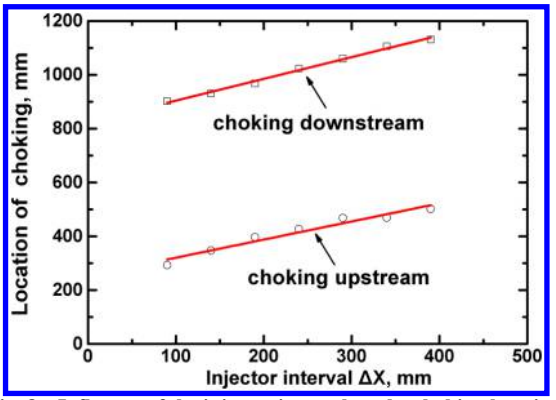

Fig. 8 Influence of the injector interval on the choking location.

240–390 mm and a rapid rise for ΔX smaller than 240 mm. This result shows that the distributed injection becomes more effective in enhancing the thrust by reducing the spacing between the first- and second-stage injectors. Combining the results from Figs. 6 and 7, an optimal range of ΔX can be within 40–240 mm to avoid the combustor unstart and a larger thrust increment.

To estimate the uncertainty in the measured thrust, experiments for $\Delta X = 190$ were repeated for three times and a 3% uncertainty was hence obtained. The uncertainty mainly comes from the measurement of the fuel flow rate, airflow rate, and air pressure. Considering that the reference thrust in the cold flow condition was overestimated due to the boundary separation at the combustor exit, thus the specific thrust increment was accordingly underestimated. Although the accurate specific thrust increment is difficult to be directly measured, it can be calculated with a corrected pressure distribution by eliminating the influence of the boundary separation. Tomioka et al. [20] proposed to use the Crocco equation [29] to fit the pressure distribution upstream of the separation point to reproduce the pressure distribution without the separation. Such a calculation is beyond the scope of the present study and merits future efforts for precise determination of the thrust.

Figure 10 shows the wall temperature distributions at different times for the case of the spacing $\Delta X = 240$ mm. Because the equivalence ratio of the pilot hydrogen is about 0.08 and its runtime is about 1.4 s, the contribution of hydrogen combustion to the wall temperature can be neglected compared with that of kerosene. The results show that the wall temperature distribution does not have a distinct difference before 4.0 s, namely, before the injection of kerosene at 4.2 s. All the wall temperature distributions are similar during the time interval of 6.0–9.0 s. Specifically, the temperature peak around 700 mm must be due to the combustion around the upstream fuel injection.

Figure 11 shows the wall temperature distribution at 9.0 s for different spacings between the two-staged injectors. As the spacing ΔX decreases, it can be seen that the wall temperatures at $x <$

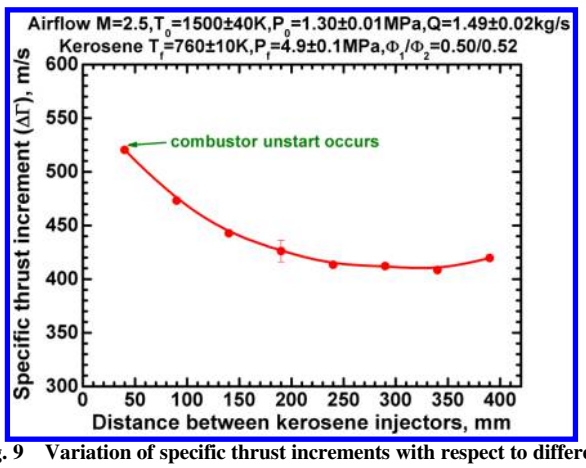

Fig. 9 Variation of specific thrust increments with respect to different spacings between the two-staged injectors.

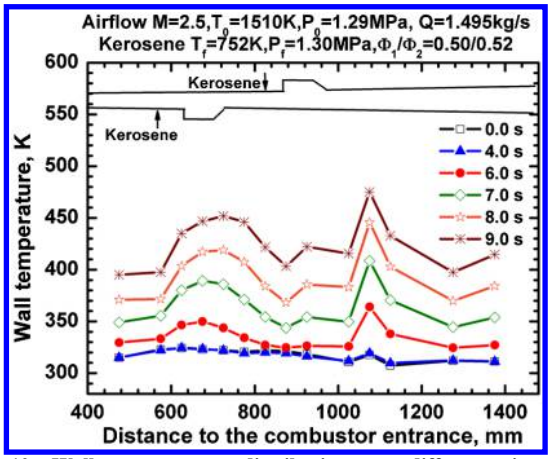

Fig. 10 Wall temperature distributions at different times for $\Delta X = 240$ mm.

900 mm decrease and the temperature peaks shift downstream, whereas the wall temperatures at $x > 900$ mm increase. This result is in accord with the understanding that distributed combustion promotes the uniformity of the wall temperature. Again, all the temperature peaks for different ΔX appear around $x = 700$ mm, corresponding to the intense combustion near the rear edge of the upstream cavity. It is interesting to note that neither small ΔX such as 40 mm nor large ΔX such as 390 mm can result in a more uniform wall temperature distribution and that the median value such as $\Delta X = 140$–240 mm can be approximately used as an optimal range of the spacing. Peak pressure downstream of the second-stage injector appeared at $x = 1070$ mm regardless of the second-stage streamwise location. The abnormal temperature spike is possibly due to a machining error (i.e., the distance between the thermocouple bead and the combustor inner wall is significantly less than the designed depth 1 mm) and, correspondingly, the measured wall temperature has a dramatic rise there. Noting that machining errors are generally difficult to detect and control, a sensitivity analysis on the effect of the distance on wall temperature measurement will be conducted numerically in a future study to determine acceptable machining errors.

B. Effect of Staged Injection on the Flame Stabilization

As discussed in the Introduction, the two-staged injection will influence the flame stabilization, which can be quantified by using the blowout limits of fuel in terms of equivalence ratio. The criterion for flame stabilization can be illuminated by examining the evolution of the static pressure during a typical experiment. Figure 12 shows the typical evolution of the pilot hydrogen pressure and the static combustion pressure at the location of $x = 800$ mm for stable

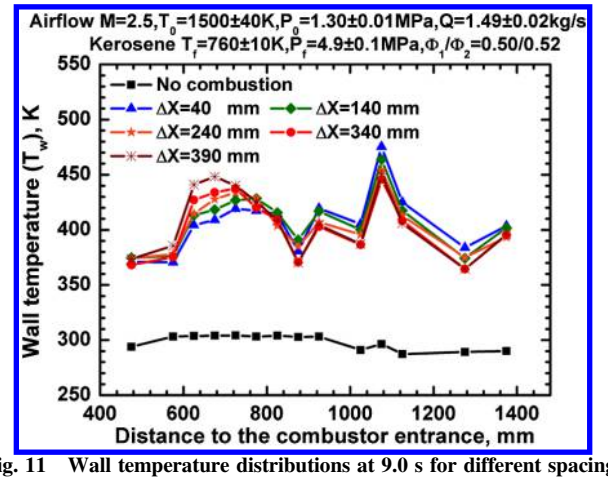

Fig. 11 Wall temperature distributions at 9.0 s for different spacings between injectors.

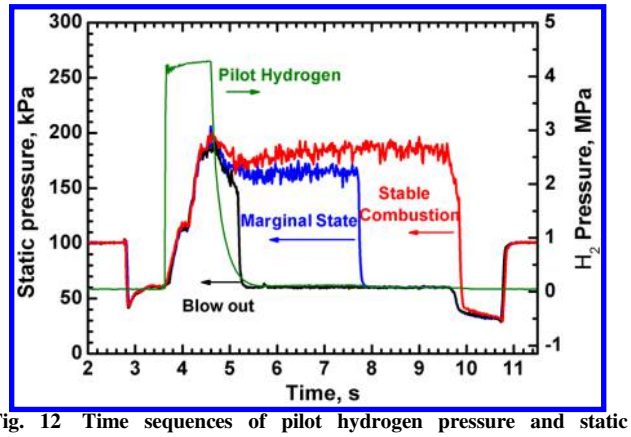

Fig. 12 Time sequences of pilot hydrogen pressure and static combustion pressure at $x = 800$ mm for cases of stable combustion, blowout, and marginal state.

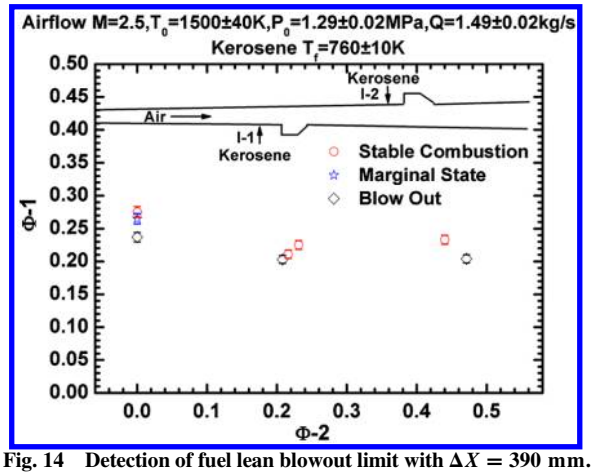

Fig. 14 Detection of fuel lean blowout limit with $\Delta X = 390$ mm.

combustion, blowout, and marginal state. The stable combustion is defined as the static pressure is maintained for at least 4.0 s after the pilot hydrogen is turned off at 5.0 s; the flame blowout is believed to occur if the static pressure immediately drops once the pilot hydrogen is turned off. The marginal state is the case in which the stable combustion stops at any intermediate moment, implying the incomplete combustion of kerosene, as shown in Fig. 12.

Figures 13 and 14 show the measured lean blowout limit of supercritical kerosene in $M = 2.5$ airflow for two typical spacings of two-staged injection, namely 190 and 390 mm. The total pressure and total temperature of the airflow are 1.29 ± 0.02 MPa and 1500 ± 40 K, respectively. The airflow rate is 1.485 ± 0.01 kg/s. It is seen that the lean blowout limit of first-stage injected fuel can substantially decrease from $\Phi_1 = 0.26$ to 0.16, as the equivalence ratio of the second-stage injected fuel Φ_2 increases to above 0.17. As discussed in the Introduction, when the two-staged fuel injectors are close to each other, the combustion around the second injector can reduce the local velocity and therefore increase the pressure. Consequently, the flame around the first injector can be stabilized for leaner combustion. It is noted that the equivalence ratio Φ_2 less than 0.2 and larger than 0.5 was not examined in the present study and could merit future study.

Figure 14 shows that the lean blowout limit of first-stage injected fuel can be decreased from 0.26 to 0.21, when Φ_2 increases to be larger than 0.20. Comparison between Figs. 13 and 14 shows that the influence of the second-stage injection on the flame stabilization decreases as the spacing ΔX increases because the interaction between the two injections becomes weaker with increase in the spacing. The present experimental result, that the influence of the second-stage injection on the flame of first-stage injection is substantial for supercritical kerosene, is different from that for hydrogen reported by Kirstein et al. [30], who found little interaction between the two-staged injections. Generally, kerosene burns more slowly than hydrogen, implying that most of the hydrogen will be reacted in the combustion zone around the first-stage injection, whereas plenty of kerosene remains to be reacted in the subsequent combustion zones. The derivation is consistent with the experimental observation that no separate peaks were in the static pressure distribution of kerosene combustion. A more well-distributed combustion of fuel along the staged injections will increase the static pressure in a stepwise way [21] and gradually slow the flow, which promotes the flame stabilization and suppresses the inlet unstart. Therefore, similar interaction between hydrogen injections can be expected for sufficiently small injector intervals compared with those in the kerosene case.

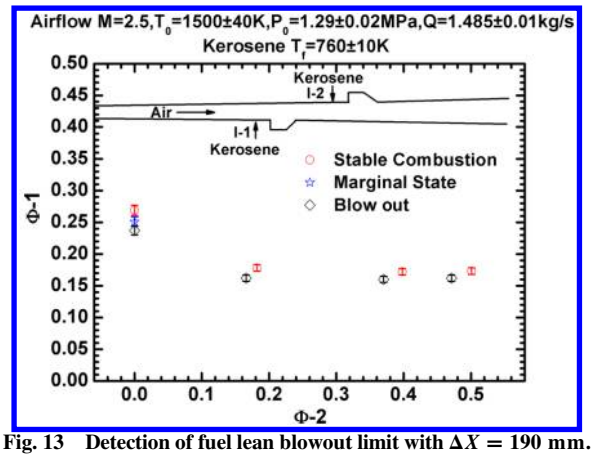

Fig. 13 Detection of fuel lean blowout limit with $\Delta X = 190$ mm.

C. Effect of Flow Rate Ratio of the Two-Staged Injection

In this subsection, the effect of the fuel flow rate ratio on the static pressure distribution, the specific thrust increment, and the wall temperature distribution will be examined for the case of $\Delta X = 190$ mm, which was identified as an optimal injector spacing. Experiments were conducted in Mach 2.5 airflows with the total pressure 1.28 ± 0.02 MPa, the total temperature 1500 ± 40 K and the airflow rate 1.48 ± 0.02 kg/s. The detailed experimental conditions are listed in Table 3.

Figure 15 shows the comparison of the normalized static pressures for three different equivalence ratio combinations with the overall equivalence ratio fixed at 1.0. The error bar in the figure denotes the extent of the pressure fluctuation. The sampling frequency of pressure transducers is 60 Hz. It can be seen that the pressures fluctuate substantially before the second-stage injector and moderately after the second-stage injector. It implies the possible existence of the low-frequency flame oscillation around the cavities. The figure shows the static pressure for the case of $\Phi_1 = 0.504/\Phi_2 = 0.527$ is

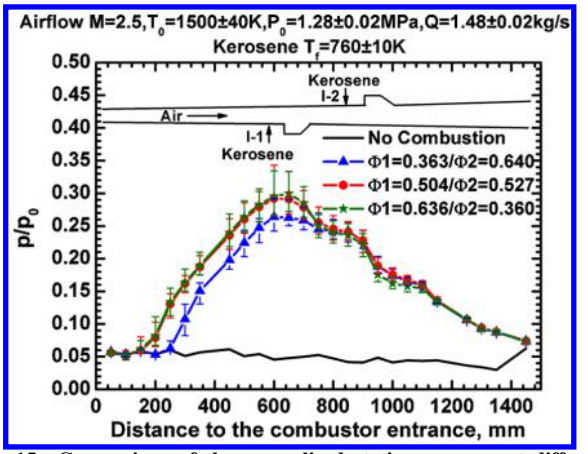

Fig. 15 Comparison of the normalized static pressures at different ratios of Φ_1/Φ_2.

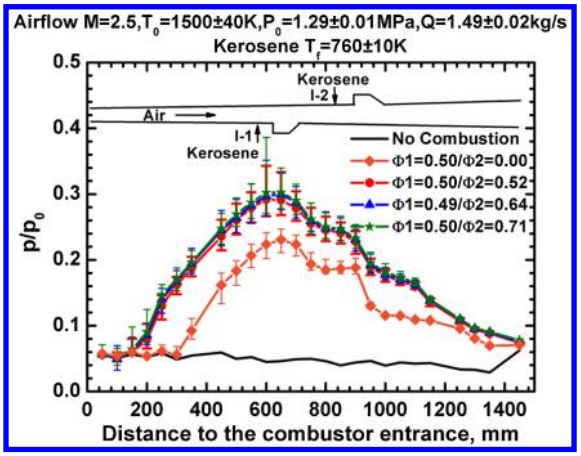

Fig. 16 Comparison of the normalized static pressures for different $\Phi_2(\Phi_1 = 0.5)$.

similar to that for $\Phi_1 = 0.636/\Phi_2 = 0.360$, with both being higher than that for $\Phi_1 = 0.363/\Phi_2 = 0.640$. The specific thrust increment listed in Table 3 has the same trend.

Figure 16 shows the comparison of the normalized static pressures for different Φ_2 and with the fixed $\Phi_1 = 0.5$. Compared with the case for $\Phi_2 = 0$, the second-stage injection causes substantial pressure rise, as it should. However, when Φ_2 is larger than 0.50, the static pressure rise shows a somewhat "saturation." It can be concluded from Figs. 15 and 16 that, for the given spacing of the two-staged injection, $\Phi_1 = 0.5/\Phi_2 = 0.5$ is an optimal combination of the fuel equivalence ratios.

IV. Conclusions

A two-staged fuel injection scheme integrated with dislocated dual cavities was proposed to enhance the overall performance of a model supersonic combustor in terms of thrust increment, combustor unstart, flame stabilization, and combustion heat release. The experiments were conducted on a direct-connect test facility for Mach 2.5 airflows with a total temperature of 1500 ± 40 K and total pressures of 1.29 ± 0.03 MPa.

The effects of the injector spacing on the static pressure distribution, the specific thrust increment, and the wall temperature distribution were first examined. The results show the high engine thrust is achieved as small injection intervals, which increases the possibility of combustion unstart and reversely reduces the wall temperature uniformity. It is optimal to obtain a high engine thrust while maintaining a uniform wall temperature and avoiding the unstart. Higher wall temperature uniformity is also favored for the design of the wall cooling system. The balanced combustor performance can be achieved by an "optimal" interval or a certain optimal range of the intervals.

The effects of the second-staged injection on the flame stabilization were investigated. The lean blowout limit of the fuel injected at the first-staged injection can be substantially decreased by increasing the equivalence ratio of the fuel injection from the second-staged injection. The stabilization effect of the second-staged injection becomes weaker for larger spacing between the two injectors.

The effects of fuel flow rate ratio of the two-staged injection on the static pressure distribution and the specific thrust increment were examined for $\Delta X = 190$ mm. The results show that $\Phi_1 = 0.5/\Phi_2 = 0.5$ is an optimal combination of the fuel equivalence ratios.

In summary, the proposed two-staged fuel injection scheme integrated with dislocated dual cavities can be used in the supersonic combustor design to optimize the combustion performance under the framework of four balanced factors (i.e., thrust increment, flame stability, inlet start, and wall cooling). Further work is of course merited to extend the present design to a wider range of flow Mach numbers.

Acknowledgments

The current research program at the Chinese Academy of Sciences was supported by the National Natural Science Foundation of China under contracts 91016005 and 10621202. The work at the Hong Kong Polytechnic University was supported in part by the Central Research grant G-UB50 under the Departmental General Research Fund Scheme. The authors would like to acknowledge G. Yu, X. S. Wei, X. N. Lu, L. J. Meng, and Y. Li for their technical support.

References

[1] Yu, G., Li, J. G., Zhao, Z., Chang, X. Y., and Sung, C. J., "Investigation of Vaporized Kerosene Injection in a Supersonic Model Combustor," *12th AIAA International Space Planes and Hypersonic Systems and Technologies*, AIAA Paper 2003-6938, 2003.

[2] Fan, X. J., Yu, G., Li, J. G., Zhang, X. Y., and Sung, C. J., "Investigation of Vaporized Kerosene Injection and Combustion in a Supersonic Model Combustor," *Journal of Propulsion and Power*, Vol. 22, No. 1, 2006, pp. 103–110.

[3] Amaya, J. A., Hunt, A. T., Colby, J. A., and Menon, S., "Thermal Effects on Fuel Injection in a Swirl-Stabilized Gas Turbine Combustor," *42nd AIAA/ASME/SAE/ASEE Joint Propulsion Conference & Exhibit*, AIAA Paper 2006-4919, 2006.

[4] Owens, M. G., Tehranian, S., Segal, C., and Vinogradov, V. A., "Flame-Holding Configurations for Kerosene Combustion in a Mach 1.8 Airflow," *Journal of Propulsion and Power*, Vol. 14, No. 4, 1998, pp. 456–461.

[5] Mathur, T., Gruber, M., Jackson, K., Donbar, J., Donaldson, W., Jackson, T., and Billig, F. S., "Supersonic Combustion Experiments with a Cavity-Based Fuel Injector," *Journal of Propulsion and Power*, Vol. 17, No. 6, 2001, pp. 1305–1312.

[6] Gruber, M. R., Donbar, J., Carter, C. D., and Hsu, K.-Y., "Mixing and Combustion Studies Using Cavity-Based Flameholders in a Supersonic Flow," *Journal of Propulsion and Power*, Vol. 20, No. 5, 2004, pp. 769–778.

[7] Gruber, M. R., Baurle, R. A., Mathur, T., and Hsu, K.-Y., "Fundamental Studies of Cavity-Based Flameholder Concepts for Supersonic Combustors," *Journal of Propulsion and Power*, Vol. 17, No. 1, 2001, pp. 146–153.

[8] Ben-Yakar, A., and Hanson, R. K., "Cavity Flame-Holders for Ignition and Flame Stabilization in Scramjets: An Overview," *Journal of Propulsion and Power*, Vol. 17, No. 4, 2001, pp. 869–877.

[9] Rasmussen, C. C., Driscoll, J. F., Carter, C. D., and Hsu, K.-Y., "Characteristics of Cavity-Stabilized Flames in Supersonic Flow," *Journal of Propulsion and Power*, Vol. 21, No. 4, 2005, pp. 765–768.

[10] Rasmussen, C. C., Dhanuka, S. K., and Driscoll, J. F., "Visualization of Flameholding Mechanisms in a Supersonic Combustor Using PLIF," *Proceedings of the Combustion Institute*, Vol. 31, No. 2, 2007, pp. 2505–2512.

[11] Cabell, K., Hass, N., Storch, A., and Gruber, M., "HIFIRE Direct-Connect Rig (HDCR) Phase I: Ground Test Results from the NASA Langley Arc-Heated Scramjet Test Facility," *17th AIAA International Space Planes and Hypersonic Systems and Technologies Conference*, AIAA Paper 2011-2248, 2011.

[12] Yu, K. H., Wilson, K. J., and Schadow, K. C., "Effect of Flame-Holding Cavities on Supersonic Combustion Performance," *Journal of Propulsion and Power*, Vol. 17, No. 6, 2001, pp. 1287–1295.

[13] Sun, M. B., Wu, H. Y., Fan, Z. Q., Wang, H. B., Bai, X. S., Wang, Z. G., Liang, J. H., and Liu, W. D., "Flame Stabilization in a Supersonic Combustor with Hydrogen Injection Upstream of Cavity Flameholders: Experiments and Simulations," *Journal of Aerospace Engineering*, Vol. 225, No. 12, 2011, pp. 1351–1365.

[14] Collatz, M. J., Gruber, M. R., Olmstead, D. T., Branam, R. D., Lin, K.-C., and Tam, C.-J., "Dual Cavity Scramjet Operability and Performance Study," *45th AIAA/ASME/SAE/ASEE Joint Propulsion Conference & Exhibit*, AIAA Paper 2009-5030, 2009.

[15] Sun, M. B., Gong, C., Zhang, S. P., Liang, J. H., Liu, W. D., and Wang, Z. G., "Spark Ignition Process in a Scramjet Combustor Fueled by Hydrogen and Equipped with Multi-Cavities at Mach 4 Flight Condition," *Experimental Thermal and Fluid Science*, Vol. 43, No. 8, 2012, pp. 90–96.

[16] Wang, J., Fan, X. J., Zhang, T. C., Yu, G., and Li, J. G., "Measurements of the Blowout Limits of Supercritical Aviation Kerosene in a Supersonic Combustor," *47th AIAA Joint Propulsion Conference*, AIAA Paper 2011-6108, 2011.

[17] Billig, F. S., Dugger, G. L., and Waltrap, P. J., "Inlet-Combustor Interface Problem in Scramjet Engines," *Proceedings of the 1st*

International Symposium on Air Breathing Engines, International Society of Air Breathing Engines, 1972.

[18] Billig, F. S., "Combustion Process in Supersonic Flow," *Journal of Propulsion and Power*, Vol. 4, No. 3, 1988, pp. 209–216.

[19] Thomas, S. R., and Guy, R. W., "Scramjet Testing from Mach 4-20 Present Capability and Needs for the Nineties," AIAA Paper 1990-1388, 1990.

[20] Tomioka, S., Murakami, A., Kudo, K., and Mitani, T., "Combustion Tests of a Staged Supersoinc Combustor with a Strut," *Journal of Propulsion and Power*, Vol. 17, No. 2, 2001, pp. 293–300.

[21] Tomioka, S., Kobayashi, K., Kudo, K., Murakami, A., and Mitani, T., "Effects of Injection Configuration on Performance of a Staged Supersonic Combustor," *Journal of Propulsion and Power*, Vol. 19, No. 5, 2003, pp. 876–884.

[22] Fan, X. J., Yu, G., Li, J. G., Lu, X. Y., and Sung, C. J., "Performance of Supersonic Model Combustors with Distributed Injection of Supercritical Kerosene," *43rd AIAA/ASME/SAE/ASEE Joint Propulsion Conference*, AIAA Paper 2007-5406, 2007.

[23] Yuan, Y. M., Yang, M., Zhang, T. C., and Fan, X. J., "Visualization of Vaporized Kerosene Combustion in a Supersonic Combustor Using Pulsed Schlieren System," *48th AIAA/ASME/SAE/ASEE Joint Propulsion Conference & Exhibit*, AIAA Paper 2012-3848, 2012.

[24] Li, J. G., Ma, F. H., Yang, V., Lin, K.-C., and Jackson, T. A., "Comprehensive Study of Ignition Transient in an Ethylene-Fueled Scramjet Combustor," *43rd AIAA/ASME/SAE/ASEE Joint Propulsion Conference & Exhibit*, AIAA Paper 2007-5025, 2007.

[25] Yu, G., Li, J. G., Zhang, X. Y., Chen, L. H., and Sung, C.-J., "Investigation on Combustion Characteristics of Kerosene-Hydrogen Dual Fuel in a Supersonic Combustor," *36th AIAA/ASME/SAE/ASEE Joint Propulsion Conference & Exhibit*, AIAA Paper 2000-3620, 2000.

[26] Fan, X. J., Zhong, F. Q., Yu, G., Li, J. G., and Sung, C. J., "Catalytic Cracking and Heat Sink Capacity of Aviation Kerosene Under Supercritical Conditions," *Journal of Propulsion and Power*, Vol. 25, No. 6, 2009, pp. 1226–1232.

[27] Heiser, W. H., and Pratt, D. T., *Hypersonic Airbreathing Propulsion*, AIAA Education Series, AIAA, Washington, D.C., 1994, PP. 347–349.

[28] Yu, G., Li, J. G., Zhao, J. R., Qian, D. X., Han, B., and Li, Y., "Hydrogen-Air Supersonic Combustion Study by Strut Injectors," *34th AIAA Joint Propulsion Conference*, AIAA Paper 1998-3275, 1998.

[29] Crocco, L., "One Dimensional Treatment of Steady Gas Dynamics," *Fundamentals of Gas Dynamics, High Speed Aerodynamics and Jet Propulsion*, Princeton Univ. Press, Princeton, NJ, 1958, pp. 105–130.

[30] Kirstein, S., Maier, D., Fuhrmann, T., Hupfer, A., and Kau, H., "Experimental Study on Staged Injection in a Supersonic Combustor," *16th AIAA/DLR/DGLR International Space Planes and Hypersonic Systems and Technologies Conference*, AIAA Paper 2009-7343, 2009.

C. Segal
Associate Editor